Changes in Electronic Structure upon Lithium Insertion into $Fe_2(SO_4)_3$ and $Fe_2(MoO_4)_3$ Investigated by X-ray Absorption Spectroscopy

Junichi Shirakawa,[†] Masanobu Nakayama,[†] Masataka Wakihara,*[,†] and Yoshiharu Uchimoto[‡]

Department of Applied Chemistry, Tokyo Institute of Technology, 2-12-1 Ookayama Megro-ku, Tokyo 152-8552, Japan, and Department of Interdisciplinary Environment, Graduate School of Human and Environmental Studies, Kyoto University, Yoshida-nihonmatsu-cho, Sakyo-ku, Kyoto 606-8501, Japan

Received: September 6, 2006; In Final Form: November 25, 2006

Changes in electronic structure upon electrochemical lithium insertion into two iron compounds, namely, rhombohedral $Fe_2(SO_4)_3$ with a NASICON-type structure and monoclinic $Fe_2(MoO_4)_3$, were investigated using X-ray absorption spectroscopy (XAS). Fe K-edge and L_{III}- and L_{II}-edge XAS revealed that the rearrangement of Fe d electrons or rehybridization of Fe d−O p bonding took place accompanied by the reduction of Fe ions upon Li insertion for both samples and that a larger change in spectra was observed in $Fe_2(SO_4)_3$. In addition, the changes in the electronic structure of the polyanion units XO_4^{2-} (X = S or Mo) after Li insertion were also investigated by O K-edge and S K-edge or Mo L_{III}-edge XAS. The results indicated that the electronic structure around oxygen markedly changed in $Fe_2(MoO_4)_3$, while no significant change was observed in $Fe_2(SO_4)_3$.

Introduction

The demand for higher energy, longer life, and lower cost cathode materials for the lithium ion battery has gradually increased since it was created. Until today, lithiated cobalt oxide, i.e., $LiCoO_2$, has been mainly used for commercial lithium ion batteries because of its good cyclability and high voltage.[1] However, since cobalt compounds are expensive, alternative cathode materials are desired for their large-scale use in the future, e.g., hybrid-type electronic vehicles (HEV). Among several candidates, iron compounds are one of the most attractive cathode materials from both the economical and environmental viewpoints. In the 1980s, Goodenough et al. investigated Li insertion into $Fe_2(XO_4)_3$ (X = S, Mo, W) with a NASICON-type or a similar type of structure by both chemical and electrochemical methods.[2,3] In addition, they also investigated various iron phosphates, olivine-type $LiFePO_4$, NASICON-type or NASICON-like $Li_3Fe_2(PO_4)_3$, and $LiFeP_2O_7$.[4−8] These compounds are classified as "polyanion compounds" that contain compact tetrahedral units, e.g., XO_4 (X = S, Mo, P, etc.) and show much higher voltages than normal oxides upon charging and discharging. It was suggested that the high cell potential observed in polyanion electrodes is related to the small covalency in the Fe−O bond.[4−8] This was arising from inductive effects where a strong polarization of O^{2-} toward the polyanion center X^{n+} leads to a weaker Fe 3d−O 2p hybridized orbital, and it results in a lowering of the energy of Fe^{2+}/Fe^{3+} redox couples. In other words, the valence d band of Fe places around the Fermi level and is isolated from the polyanion band. This simple description of the electronic structure for polyanion compounds could account for the observed high voltage. To understand the mechanism of such unique electronic structure observed in polyanion compounds, we investigated the changes in the electronic structure around each atom of $Li_{1-x}CoPO_4$ using X-ray absorption spectroscopy (XAS).[9,10] It was demonstrated that the changes in electronic structure around the PO_4 polyanion took place accompanied by the oxidation of Co ions, although the electrons of the PO_4 polyanion were generally considered not to contribute to the oxidation. In addition, we also revealed that the polarization effect introduced by Li ions influenced changes in the electronic structure of the PO_4 polyanion. Augustsson et al. performed soft X-ray absorption and X-ray emission spectroscopy of $LiFePO_4$ and $FePO_4$.[11] They have reported that the bonding character of Fe−O changes from nonbonding to stronger hybridization with Li removal. Similar observations have been reported for Li insertion into monoclinic $Li_3Fe_2(PO_4)_3$ using XAS and ab initio calculation, and it revealed that the charge compensation occurred around polyanion, PO_4, as is the case of olivine type material.[12] Therefore, it has been presumed that electronic structure around polyanion units, XO_4, varies upon Li insertion or removal as well as other transition metal compounds.[13−19] However, to our knowledge, no investigation of the electronic structure of polyanion compounds other than those with PO_4 has been reported.

Thus, in this study, we have investigated the electronic structure of polyanion compounds with different polyanion centers, namely $Fe_2(SO_4)_3$ and $Fe_2(MoO_4)_3$, and their lithiated samples by using XAS technique. By comparison of the difference in electronic structure among them, the relationship between polyanion centers and their electrochemical property would be clarified.

Structural Description

Figure 1 represents the crystal structures of $Fe_2(SO_4)_3$ and $Fe_2(MoO_4)_3$ reported elsewhere.[2,4] Although $Fe_2(SO_4)_3$ and $Fe_2(MoO_4)_3$ belong to different crystal systems (the former has rhombohedral and the latter monoclinic symmetry, respectively), the framework of $Fe_2(SO_4)_3$ and $Fe_2(MoO_4)_3$ can be described commonly as follows: FeO_6 octahedra and XO_4 polyanion tetrahedra are three-dimensionally placed by sharing a corner with oxygen atoms. In addition, these compounds could insert

* To whom correspondence should be addressed. E-mail: mwakihar@o.cc.titech.ac.jp.
[†] Tokyo Institute of Technology.
[‡] Kyoto University.

10.1021/jp065802g CCC: $37.00
Published on Web 01/24/2007

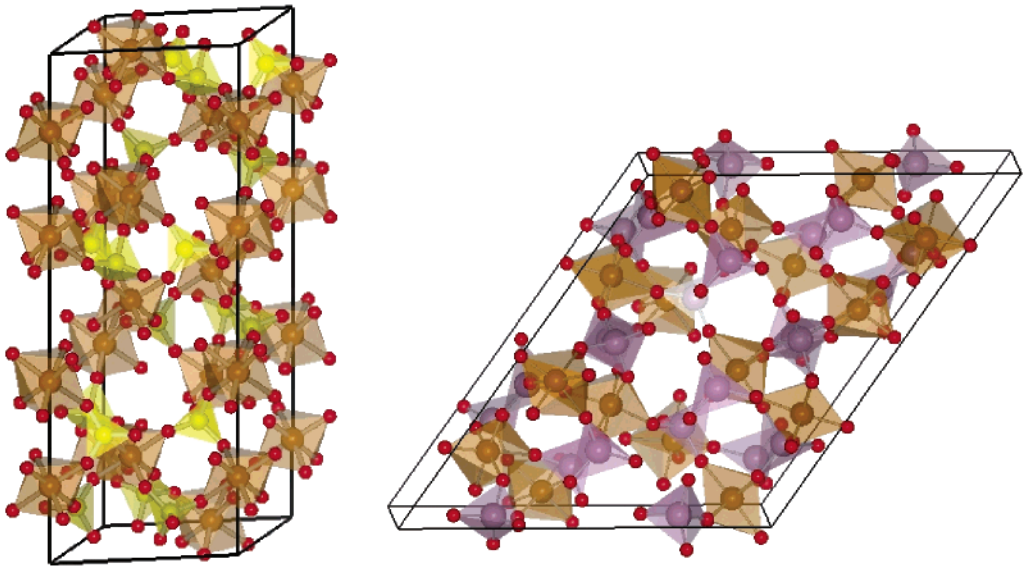

Figure 1. Crystal structure of (left) $Fe_2(SO_4)_3$ with NASICON-type rhombohedral structure (space group $R\bar{3}$) and (right) $Fe_2(MoO_4)_3$ with monoclinic structure (space group $P2_1$).

2 mol of Li at its maximum due to the limitation of the amount of the redox couple, Fe^{3+}/Fe^{2+}.[3,4]

Experimental Section

Rhombohedral $Fe_2(SO_4)_3$ was synthesized by using commercial $Fe_2(SO_4)_3 \cdot nH_2O$ (High Purity Chem. Co., Ltd., 99% up) as starting material. $Fe_2(SO_4)_3 \cdot nH_2O$ was dehydrated by heating at 250 °C for 12 h in air and crystallized by heating in a vacuum quartz tube at 600 °C for 12 h.[4] All experiments for $Fe_2(SO_4)_3$ were performed in Ar atmosphere because of its deliquescence. Monoclinic $Fe_2(MoO_4)_3$ was synthesized by a citric acid complex method using $Fe(NO_3)_3 \cdot 9H_2O$ and $(NH_4)_6Mo_7O_{24} \cdot 4H_2O$ as starting materials. All materials each in a stoichiometric ratio were solved into extrapure water and mixed together. Then, excessive citric acid which is about 50% more than the stoichiometric amount of each metal was slowly added to the solution with stirring on a hot plate. After evaporation of the solvent, the target product was obtained by sintering twice at 650 °C for 12 h. The phase identification and refinement of the lattice parameters for the samples were performed by powder X-ray diffraction (XRD) analysis using Cu Kα radiation (RINT-2500V, Rigaku Co., Ltd.). In the case of $Fe_2(MoO_4)_3$, Rietveld refinement was carried out using the RIETAN program.[20]

Electrochemical Li insertion into $Fe_2(XO_4)_3$ (X = S, Mo) was performed using a three-electrode cell. The working electrode was prepared using a mixture of 70 wt % active materials, 25 wt % acetylene black as a current collector, and 5 wt % polyvinylidene fluoride (PVdF) binder. Li foil (Aldrich) was used as a counter electrode and a reference electrode. The electrolyte used was 1 M $LiClO_4$ dissolved in ethylene carbonate/diethyl carbonate (volume ratio of 1:1) (Tomiyama Pure Chemical Industries Co., Ltd.). Li insertion was carried out at 0.1, 0.2, and 1 C, where 1 C corresponds to 67.02 mA g^{-1} for $Fe_2(SO_4)_3$ and 45.31 mA g^{-1} for $Fe_2(MoO_4)_3$, respectively. Discharge cutoff voltages were set at 3.2 V for $Fe_2(SO_4)_3$ and 2.5 V for $Fe_2(MoO_4)_3$, respectively.

Fe K-edge XAS was performed by a transmission method using synchrotron radiation at the beamline BL-7C, Photon Factory (PF), High-energy Accelerator Research Organization in Tsukuba, Japan. The absorption of the Cu K-edge was used to calibrate the absolute energy scale. XAS within the soft X-ray region was carried out using synchrotron radiation at the beamlines BL-11A for the Fe L-edge and O K-edge and BL-11B for the Mo L_{III}-edge, respectively, in PF. The absorption of X-ray was determined by the total-electron-yield method. The total electron yield was divided by the storage-ring current that was recorded simultaneously. The absorption energy was calibrated by comparison with data for the standard materials Fe_2O_3, S, and MoO_3. For the samples after electrochemical treatment, all installation operations were performed in N_2 atmosphere.

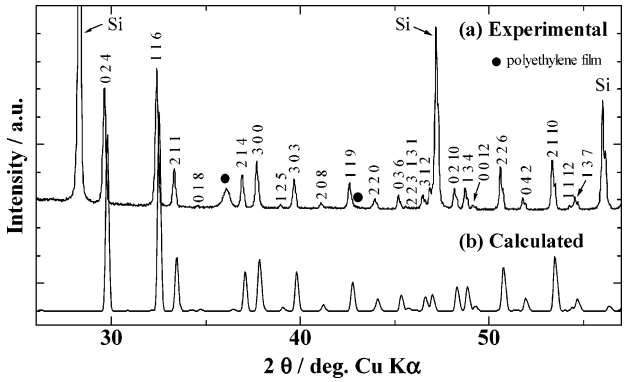

Figure 2. XRD patterns of $Fe_2(SO_4)_3$. Si powder was mixed as an internal standard.

Results and Discussion

Figure 2 shows the XRD patterns of obtained $Fe_2(SO_4)_3$ with simulated patterns whose structural parameters were cited from previous reports.[21] All Bragg peaks can be identified by appropriate reflection indices without any impurity peaks; therefore, the obtained $Fe_2(SO_4)_3$ belonged to NASICON-type rhombohedral lattice (space group; $R\bar{3}$) with the crystal frameworks as shown in Figure 1. Rietveld refinement was not performed for $Fe_2(SO_4)_3$ phase, since the peaks and background of polyethylene film covering the samples to prevent the sample from deliquescence made the fitting difficult. Instead, the lattice parameters were refined using Si powder as an internal standard, and the results ($a = 8.2354(3)$ Å, $c = 22.179(1)$ Å) agreed well with those of previous reports.[21] In the case of $Fe_2(MoO_4)_3$, Rietveld refinement using a monoclinic lattice (space group;

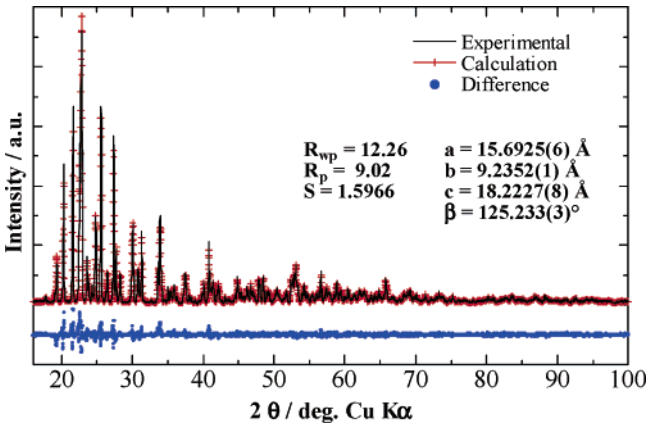

Figure 3. Result of Rietveld refinement of synthesized $Fe_2(MoO_4)_3$. The atomic positions of each atom were fixed to those of reference data.[22]

$P2_1$) was performed, and the result was shown in Figure 3. The positions of each atom were fixed to those of previous paper,[22] which could be enough for the purpose of the refinement for the lattice parameters. The obtained lattice parameters (a = 15.6925(6) Å, b = 9.2352(1) Å, c = 18.2227(8) Å, β = 125.233(3) Å) showed good agreement with those of the previous papers.[22]

SEM images of $Fe_2(SO_4)_3$ and $Fe_2(MoO_4)_3$ are shown in Figure 4. The irregular polyhedral fine particles were obtained with primary size of ~2 μm. $Fe_2(MoO_4)_3$ particles seem to be partially aggregated with each other; on the contrary, no clear aggregation is observed for $Fe_2(SO_4)_3$ particles.

The discharge curves of $Fe_2(SO_4)_3$ and $Fe_2(MoO_4)_3$ under several current density conditions were shown in Figure 5. The observed discharge voltages were ~3.5 V for $Fe_2(SO_4)_3$ and ~3.0 V for $Fe_2(MoO_4)_3$, respectively, and the values were consistent with previous report.[4] In the present study, only 1 mol of Li inserted in $Fe_2(SO_4)_3$ even at 0.1 C, although approximately 2 mol of Li insertion has been reported in a previous study.[4] This discrepancy is still uncertain. One can see the amounts of electrochemically inserted Li into $Fe_2(SO_4)_3$ strongly depended on current density as shown in Figure 5,[4] and relatively larger polarization was observed with increasing current density. Thus, the undesirable side reaction would prevent the smooth lithium insertion process. Considering that the lattice parameters of $Fe_2(SO_4)_3$ were consistent with those of the sample in the previous paper,[22] the discrepancy of composition would not be significant. We infer that an inactive surface film formation due to residual water may cause the lowering of the capacity. Thus, optimization of the synthesis procedure may be needed. On the other hand, the rate performance of $Fe_2(MoO_4)_3$ was excellent compared with $Fe_2(SO_4)_3$, and the amount of Li inserted into $Fe_2(MoO_4)_3$ was close to 2 mol agreeing with the result of previous reports.[2,3,23] In addition, the cell voltage of Li insertion into $Fe_2(MoO_4)_3$ was kept constant at almost all Li contents, indicating that Li insertion proceeded under two-phase coexistence, as is in the previous reports.[2,3,22] The voltage curves of $Fe_2(SO_4)_3$ appeared relatively flat, which may suggest a two-phase coexistence. However, it is generally difficult to determine whether the reaction proceeds a single phase or a two-phase coexistence manner only by voltage profile. To our knowledge, the evidence of the two-phase coexistence in the $Li_xFe_2(SO_4)_3$ system has not been clearly reported, though a two-phase coexistent reaction was suggested in previous papers.[4,24] To clarify the variation in crystal structure during Li insertion, the XRD measurements of $Fe_2(SO_4)_3$ and $Fe_2(MoO_4)_3$ with various Li contents were carried out (Figure 6). In the case of $Fe_2(MoO_4)_3$, the two-phase coexistence manner between monoclinic and orthorhombic (space group, *Pbcn*) phases was clearly shown from the comparison with the simulated pattern of the orthorhombic phase whose structural parameters were cited from the previous report;[25] some new peaks (e.g., peaks A−D in $Li_{2.0}Fe_2(MoO_4)_3$) appeared during the lithiation, while the diffraction peaks of the monoclinic phase (e.g., well-characterized peaks E−I) faded or disappeared. After delithiation from $Li_2Fe_2(MoO_4)_3$, the XRD pattern returned to the initial monoclinic lattice, indicating that the Li insertion/removal of $Fe_2(MoO_4)_3$ reversibly occurred between the monoclinic $P2_1$ framework and the orthorhombic *Pbcn* framework. (Note that the topology of the $Fe_2(MoO_4)_3$ framework does not change before and after lithiation, although the space groups for them are different.) As is the case of $Fe_2(MoO_4)_3$, the changes in XRD patterns for $Fe_2(SO_4)_3$ upon discharging and charging indicated that the reaction reversibly proceeded with a two-phase coexistence manner. The additional peaks appeared as indicated by arrows in figure and increased in the intensity by lithium insertion. Note that the peaks of $Fe_2(SO_4)_3$ do not disappear after full discharging, indicating that the core of $Fe_2(SO_4)_3$ particles did not completely react with lithium as mentioned above. Thus, the nominal lithium amount x in $Li_xFe_2(SO_4)_3$ would be limited to ~1.0 mol at 0.1 C as indicated in Figure 5. Lithium contents of lithiated phase after phase transformation would be ~2 mol as expected in the previous report.[4,24] The structure of lithiated phase, however, could not be identified in this study. Further investigation is needed to clarify this. We refer the lithiated samples as $Li_xFe_2(MoO_4)_3$ and $Li_xFe_2(SO_4)_3$ in this paper; however. these samples exist in two-phase coexistence, maybe as $(1-x)$ $Fe_2(MoO_4)_3$ $-$ x $Li_2Fe_2(MoO_4)_3$ and $(1-x)$ $Fe_2(SO_4)_3$ $-$ x $Li_2Fe_2(SO_4)_3$ systems.

Figure 7 shows the variation of Fe K-edge XAS for $Li_xFe_2(SO_4)_3$ and $Li_xFe_2(MoO_4)_3$ during Li insertion. The absorption energies of these compounds were summarized in Table 1 and compared with those of Fe_2O_3 and FeO. Before Li insertion, the valence state of Fe ions was +3 in both compounds, since the absorption energy was close to that of Fe_2O_3. In the spectra of $LiFe_2(SO_4)_3$ and $Li_2Fe_2(MoO_4)_3$, the absorption energy shifted to lower value and agreed with that of FeO, as shown in Table 1. Therefore, the oxidation state of Fe decreased from +3 to +2 upon Li insertion. However, in the case of the spectrum of $LiFe_2(SO_4)_3$, the white line was split into two. Probably, the reduction of Fe^{3+} was not completed as mentioned above, because of two-phase coexistence, $Fe_2(SO_4)_3$ and $Li_2Fe_2(SO_4)_3$. In Figure 8, the variations of the Fe L-edge spectra for $Fe_2(SO_4)_3$ and $Fe_2(MoO_4)_3$ before and after Li insertion are represented. In the spectra of both samples, Fe L_{III}- and L_{II}-edge absorptions were observed ranging from ca. 707 to 716 eV and from ca. 721 to 727 eV, respectively. These spectra corresponded to dipole transitions from Fe $2p_{3/2}$ (L_{III}) and $2p_{1/2}$ (L_{II}) core electrons to an unoccupied 3d state ($2p^63d^n \rightarrow 2p^5$-$3d^{n+1}$), respectively. The absorption energy shifted toward the lower energy side in both L_{III} and L_{II} XAS after Li insertion, as is the case of Fe K-edge spectra. This indicates the decrease in the effective nuclear charges of the Fe ions, or Fe ions reduced. Both L_{III}- and L_{II}-edge absorptions consist of two peaks mainly, representing the intense $2p_{3/2}$, $2p_{1/2} \rightarrow$ 3d electron transition. The peak split arises from the interplay of crystal field and electronic interactions.[11] The intensity ratio of two peaks in either the L_{III}- or L_{II}-edge markedly changed after Li insertion into both compounds. According to the literature,[26] the typical

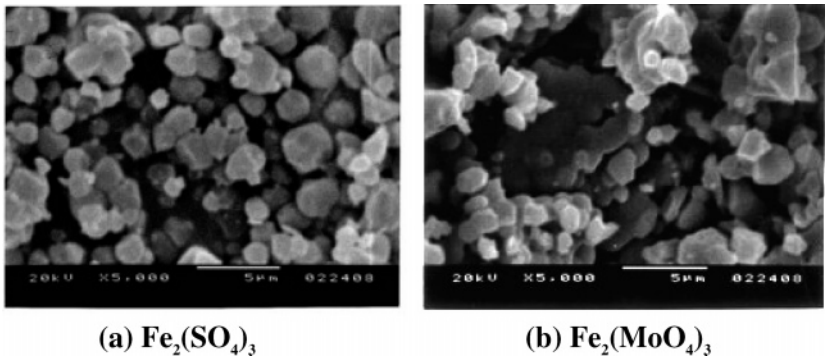

Figure 4. SEM images of (a) $Fe_2(SO_4)_3$ and (b) $Fe_2(MoO_4)_3$.

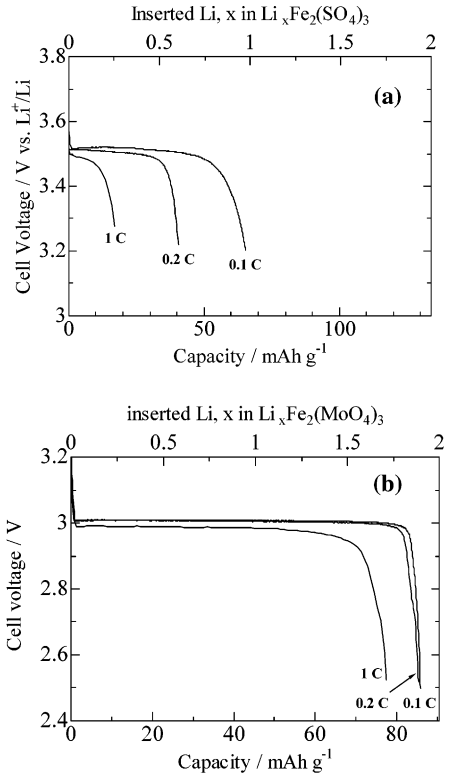

Figure 5. Variation of discharge curves of (a) $Fe_2(SO_4)_3$ and (b) $Fe_2(MoO_4)_3$ with current density.

L_{III} absorption edge of Fe^{2+} in an octahedral crystal field consists of a larger and a smaller intensity peaks at lower and higher energy region (peaks A and B in Figure 8), respectively. On the other hand, that of Fe^{3+} is described by opposite manner.[26] This supports the results in Figure 8; that is to say, the reduction of Fe^{3+} proceeded to Fe^{2+} upon Li insertion. Table 2 represents the ratio of the peak area A and B fitted by Gaussian combolution before and after lithium insertion into both compounds. As seen in the table, larger increase in the ratio of peak A and B for $Fe_2(SO_4)_3$ is indicated, although the molar amount of inserted lithium ions in $Fe_2(SO_4)_3$ is smaller than in $Fe_2(MoO_4)_3$. Note that the spectrum of $LiFe_2(SO_4)_3$ consisted of two phases, nonreacted $Fe_2(SO_4)_3$ and lithiated $Li_2Fe_2(SO_4)_3$ (Figure 6). Thus, the present results of peak separation (Table 2) did not directly relate to the intrinsic physical property. However, one can see the larger peak ratio change in $Li_xFe_2(SO_4)_3$ system despite the smaller amount of lithium insertion. Therefore, it would be concluded that larger electronic structural change occurred around Fe ions during Li removal in the $Li_xFe_2(SO_4)_3$ system than in the $Li_xFe_2(MoO_4)_3$ system. In our previous study about $Li_3Fe_2(PO_4)_3$,[12] such a spectral change was related to the rehybridization of Fe−O bonding and changes in electronic configuration among Fe d orbitals after Li insertion, which was investigated from Fe L-edge XAS and ab initio calculation. Especially, from the comparison of the results of ab initio calculation between GGA and LDA+U, it was revealed that the electronic rearrangement in the Fe d orbitals upon Li insertion were connected to the effects for localization of the d electrons, in other words, the bonding character of Fe−O hybridized orbital. These results were supported by the previous studies of other polyanion-type cathode materials.[11,27,28] Therefore, it is suggested that the changes in the intensity ratio of two peaks after Li insertion into both $Fe_2(SO_4)_3$ and $Fe_2(MoO_4)_3$ were related to the rehybridization of Fe−O bonding or rearrangement of electronic configuration in Fe d orbitals. In addition, from the difference of the changes in Fe L-edge XAS between two compounds, the variation of changes in electronic configuration in Fe d orbital or rehybridization with oxygen would be more marked in $Fe_2(SO_4)_3$ than those in $Fe_2(MoO_4)_3$ as shown in Table 2. The more detailed discussion will be shown below taking the O K-edge XAS into consideration.

The changes in the electronic structure of the polyanion units, SO_4 or MoO_4 tetrahedra, before and after Li insertion were investigated using O K-edge, S K-edge, and Mo L_{III}-edge XAS. O K-edge XAS of $Li_xFe_2(SO_4)_3$ ($x = 0$, 1) and $Li_xFe_2(MoO_4)_3$ ($x = 0$, 2) are shown in Figure 9. In the spectra of $Li_xFe_2(SO_4)_3$ ($x = 0$, 1), there are two distinct peaks, A and B, that correspond to electron transitions from O 1s to O 2p−Fe 3d hybridized orbital and O 2p−Fe or S 4sp unoccupied hybridized orbital, respectively. The peak A in $Li_xFe_2(SO_4)_3$ is rather small due to the inductive effect; that is to say, the strong covalence bonding between O 2p and S 3p leads to a small hybridization of Fe 3d−O 2p. After Li insertion into $Fe_2(SO_4)_3$, no remarkable change was observed in the spectra. Although the spectrum of $LiFe_2(SO_4)_3$ included the contribution of both $Fe_2(SO_4)_3$ and $Li_2Fe_2(SO_4)_3$ phases, almost no changes in peak width and position was indicated before and after Li insertion. Therefore, it could be concluded that the electronic structure around oxygen including the Fe 3d−O 2p hybridized orbital did not vary the electrochemical reaction. In other words, the drastic change in the peak ratio of Fe L_{III}-edge spectra of $Fe_2(SO_4)_3$ upon Li insertion would be due to the changes in electronic configuration in Fe 3d orbitals rather than the rehybridization of Fe−O bonding, which was indicated in $Li_xFe_2(MoO_4)_3$ and $Li_{3+x}Fe_2(PO_4)_3$.[12] To our knowledge, the O K-edge XAS for electrode materials of LIB show drastic spectral changes upon Li insertion/removal, especially for transition metal (TM) d−O 2p hybridized orbital. This would indicate that Li insertion into various compounds leads to the changes in the electronic structure around the oxygen ion via hybridization between TM d and O 2p orbital.[13−19] Note that the spectral changes were indicated

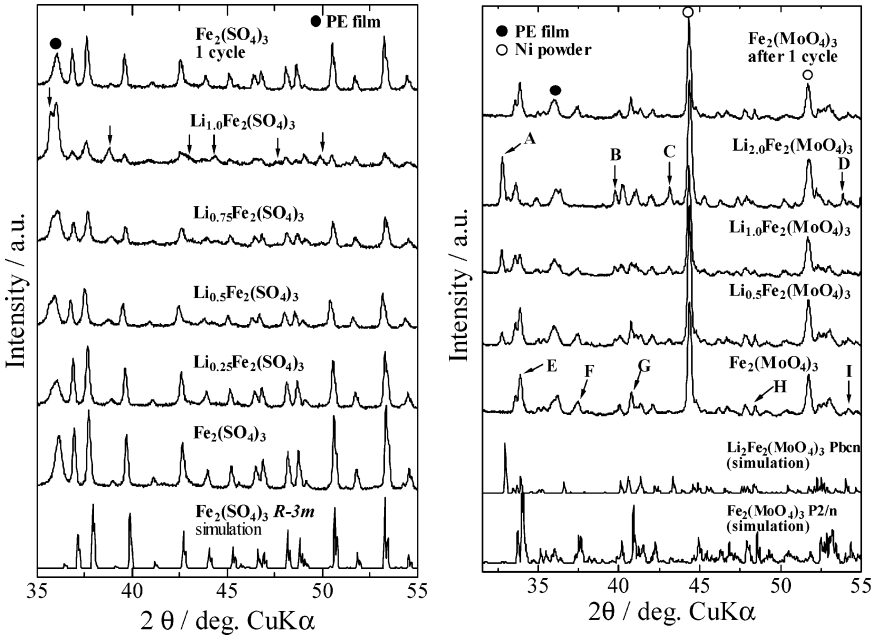

Figure 6. Variations in XRD patterns of (left) $Li_xFe_2(SO_4)_3$ and (right) $Li_xFe_2(MoO_4)_3$ upon discharge/charge cycle.

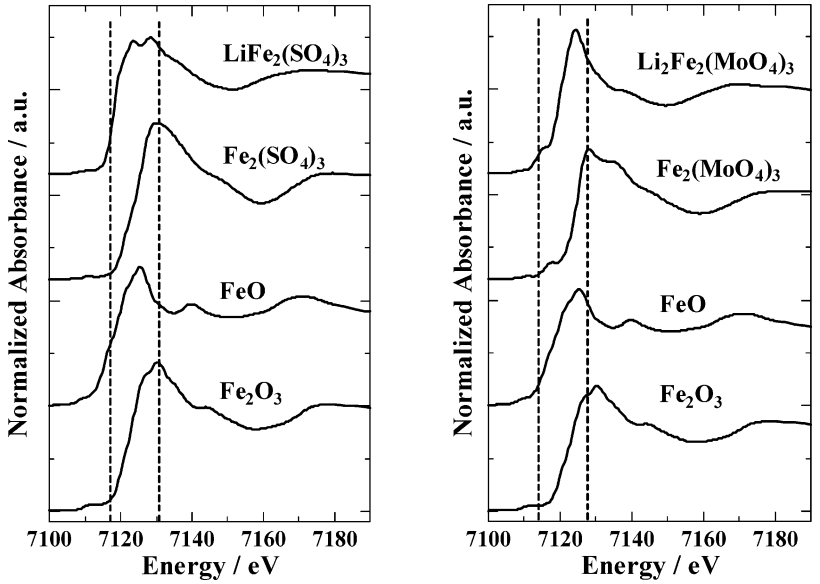

Figure 7. Variations in Fe K-edge XAS of (left) $Li_xFe_2(SO_4)_3$ ($x = 0$, 1) and (right) $Li_xFe_2(MoO_4)_3$ ($x = 0$, 2) with references, FeO and Fe_2O_3.

TABLE 1: Variation in Absorption Energy of Fe K-Edge for $Fe_2(SO_4)_3$ and $Fe_2(MoO_4)_3$ before and after Li Insertion

compds	abs energy/eV
$Fe_2(SO_4)_3$	7125.3
$LiFe_2(SO_4)_3$	7119.9
$Fe_2(MoO_4)_3$	7125.0
$Li_2Fe_2(MoO_4)_3$	7120.7
Fe_2O_3	7124.7
FeO	7120.7

even in the case of olivine-type $LiMPO_4$ (M = Fe, Co) and $Li_3Fe_2(PO_4)_3$ where the inductive effect weakens hybridization between TM d and O 2p orbital.[9−12] Therefore, no marked changes in peak A for $Li_xFe_2(SO_4)_3$ indicated that the strong ionic character of Fe 3d−O 2p bonding due to the large inductive effect caused by SO_4 tetrahedra kept the electronic structure around oxygen unchanged by electrochemical lithiation, and oxygen ions hardly contributed to the charge compensation upon Li insertion.

On the other hand, the O K-edge spectral change for $Li_xFe_2(MoO_4)_3$ was quite different from that for $Li_xFe_2(SO_4)_3$. There are three peaks, C−E, in the spectrum of $Fe_2(MoO_4)_3$. Peaks C and D corresponds to the electron transition from the O 1s orbital to the Fe 3d−O 2p or Mo 4d−O 2p hybridized orbital, and peak E assigned as the transition to O 2p−TM sp hybridized orbital. The peaks C and D for $Fe_2(MoO_4)_3$ are apparently larger than the peak A for $Fe_2(SO_4)_3$. This would be caused by the large covalent bonding of Mo 4d and/or Fe 3d with O 2p orbital. After Li insertion into $Fe_2(MoO_4)_3$, the intensity of peak C decreased, and absorption energy shifted toward lower energy side. Thus, it reveals that the TM d and O 2p hybridized orbital involved the electron-transfer process during lithiation. In addition, a new peak F appeared after Li insertion, indicating the electrostatic interaction between inserted Li and the O 2p orbital as reported in previous papers.[15,16,29]

As mentioned above, the O K-edge spectral changes are different between $Li_xFe_2(SO_4)_3$ and $Li_xFe_2(MoO_4)_3$, although both polyanion centers consist of a sixth valent element. To

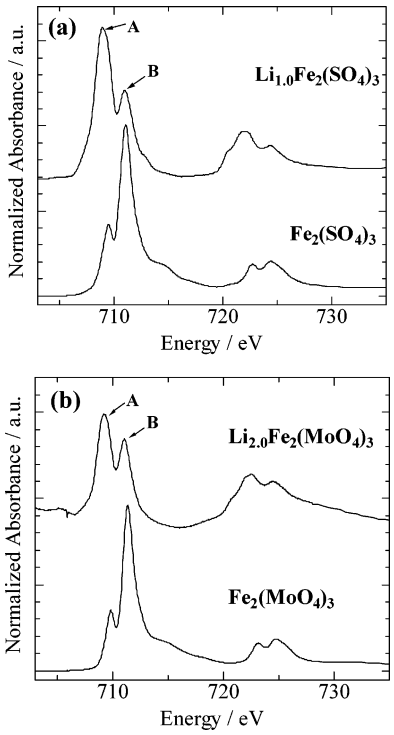

Figure 8. Variations in Fe L_{III}- and L_{II}-edge XAS profiles of (a) Li_x-$Fe_2(SO_4)_3$ ($x = 0$, 1) and (b) $Li_xFe_2(MoO_4)_3$ ($x = 0$, 2).

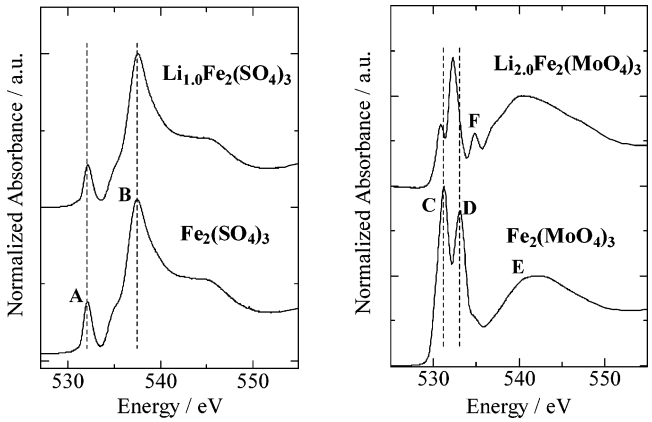

Figure 9. Variations in O K-edge XAS profiles of (left) $Li_xFe_2(SO_4)_3$ ($x = 0$, 1) and (right) $Li_xFe_2(MoO_4)_3$ ($x = 0$, 2).

TABLE 2: Gaussian Fitting of Ratio of Peak A to Peak B in Fe L_{III}-Edge XAS Profiles of $Li_xFe_2(SO_4)_3$ ($x = 0$, 1) and $Li_xFe_2(MoO_4)_3$ ($x = 0$, 2)

compds	ratio of peak A/B
$Fe_2(SO_4)_3$	0.160
$LiFe_2(SO_4)_3$	1.833
$Fe_2(MoO_4)_3$	0.147
$Li_2Fe_2(MoO_4)_3$	1.419

clarify the origin of difference in the O K-edge spectral change, S K-edge and Mo L_{III}-edge XAS were measured for Li_xFe_2-$(SO_4)_3$ and $Li_xFe_2(MoO_4)_3$, respectively. Figure 10 presents the results of the S K-edge and Mo L_{III}-edge XAS for $Li_xFe_2(SO_4)_3$ ($x = 0$, 1) and $Li_xFe_2(MoO_4)_3$ ($x = 0$, 2), respectively. Two peaks were observed in the S K-edge spectra of $Fe_2(SO_4)_3$: (1) the main absorption peak at ~2482 eV due to the transition from S 1s to S 3p; (2) a weak preedge peak at ~2470 eV. In previous studies, a preedge peak was observed in S K-edge XAS for $CuSO_4$, whereas S K-edge XAS for $ZnSO_4$ did not show such a preedge peak.[30,31] This would indicate that the state of

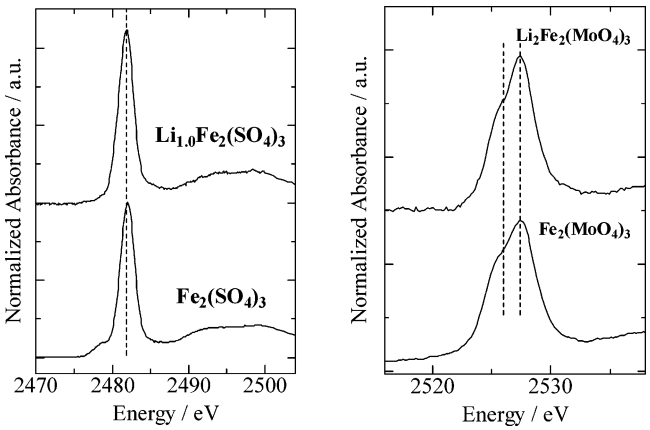

Figure 10. Variations in (left) S K-edge XAS profiles of $Li_xFe_2(SO_4)_3$ ($x = 0$, 1) and (right) Mo L_{III}-edge XAS for $Li_xFe_2(MoO_4)_3$ ($x = 0$, 2).

the TM d orbital and/or the number of d electrons affects the change in the electronic structure of sulfur via oxygen ions.[30,31] Therefore, a similar interaction between Fe^{3+} and SO_4^{2-} would take place, resulting in the appearance of weak preedge peak. The preedge peak disappeared after Li insertion, indicating changes in the interaction between Fe 3d and SO_4 tetrahedra due to the increase in the number of d electrons around Fe ions. However, the electronic structure around sulfur ions hardly changed except for the disappearance of preedge peak, and the absorption energy of the main peak was kept at constant after Li insertion. In the Mo L_{III}-edge spectrum in which electron transition took place from the Mo $2p_{3/2}$ orbital to the 4d orbital, two peaks were observed, corresponding to interplay of crystal field (tetrahedral symmetry of MoO_4) and electronic interactions. As is the case of S K-edge spectra, no remarkable changes in spectra were observed before and after Li insertion into Fe_2-$(MoO_4)_3$. Accordingly, there were almost no influences of Li insertion on the electronic structure around sulfur and molybdenum ions. This results indicate that the changes in O K-edge XAS for $Li_xFe_2(MoO_4)_3$ relates to the rehybridization of Fe 3d−O 2p orbital.

In a summary of the results of XAS, less Fe−O hybridization is indicated in $Li_xFe_2(SO_4)_3$ than in $Li_xFe_2(MoO_4)_3$, although both of the valence state for the polyanion center are +6. Therefore, one can see the fact that the electronic structure around oxygen and its change during Li insertion/removal are strongly dependent on the polyanion center. The cell voltage of $Li_xFe_2(SO_4)_3$ is much higher than that of $Li_xFe_2(MoO_4)_3$, since the Fe 3d orbital remains isolated from oxide ion, or higher the ionic character of Fe ions, in $Li_xFe_2(SO_4)_3$.

Conclusions

In this study, we investigated the changes in electronic structure for Li insertion into rhombohedral $Fe_2(SO_4)_3$ with NASICON-type and monoclinic $Fe_2(MoO_4)_3$. The single phases of both $Fe_2(SO_4)_3$ and $Fe_2(MoO_4)_3$ were obtained, and electrochemical reaction proceeded in a two-phase coexistence manner from the results of XRD. By Fe K-edge and L-edge XAS, the reduction of Fe^{3+} to Fe^{2+} was confirmed in both samples during Li insertion. In addition, in the case of $Fe_2(SO_4)_3$, larger changes in Fe L-edge spectra were observed during Li insertion compared with that of $Fe_2(MoO_4)_3$, and no marked change in O K-edge XAS was observed. Therefore, the rearrangement of electronic configuration among Fe 3d orbitals mainly took place in $Li_2Fe_2(SO_4)_3$, and electrons around oxygen do not contribute to the electronic transfer. On the other hand, peak shift and

additional peak appearance were observed in Fe−O hybridized orbital during lithium insertion into $Fe_2(MoO_4)_3$. S K-edge and Mo L_{III}-edge XAS showed almost no marked changes after Li insertion, indicating little contribution to charge compensation. The difference in spectral changes for Fe and O between both compounds could be ascribed to the inductive effect of polyanion center of S^{6+} or Mo^{6+}. Although the formal oxidation state of S^{6+} and Mo^{6+} is the same, a stronger covalent bond forms in the SO_4 unit, leading to larger ionic character in Fe ions of $Li_2Fe_2(SO_4)_3$. This would be associated with higher cell voltage in $Fe_2(SO_4)_3$ upon Li insertion than in $Fe_2(MoO_4)_3$.

Acknowledgment. J.S. thanks the Japan Society for the Promotion of Science (JSPS) for financial support. Figure 1 is described using VICS developed by R. A. Dilanian and F. Izumi.

References and Notes

(1) Mizushima, K.; Jones, P. C.; Wiseman, P. J.; Goodenough, J. B. *Mater. Res. Bull.* **1980**, *15*, 783.
(2) Manthiram, A.; Goodenough, J. B. *J. Solid State Chem.* **1987**, *71*, 349.
(3) Manthiram, A.; Goodenough, J. B. *J. Power Sources* **1989**, *26*, 403.
(4) Nanjundaswamy, K. S.; Padhi, A. K.; Goodenough, J. B.; Okada, S.; Ohtsuka, H.; Arai, H.; Yamaki, J. *Solid State Ionics* **1996**, *92*, 1.
(5) Padhi, A. K.; Nanjundaswamy, K. S.; Goodenough, J. B. *J. Electrochem. Soc.* **1997**, *144*, 1188.
(6) Padhi, A. K.; Nanjundaswamy, K. S.; Masquelier, C.; Okada, S.; Goodenough, J. B. *J. Electrochem. Soc.* **1997**, *144*, 1609.
(7) Padhi, A. K.; Nanjundaswamy, K. S.; Masquelier, C.; Goodenough, J. B. *J. Electrochem. Soc.* **1997**, *144*, 2581.
(8) Goodenough, J. B.; Manivannan, V. *Denki Kagaku* **1998**, *66*, 1173.
(9) Nakayama, M.; Goto, S.; Uchimoto, Y.; Wakihara, M.; Kitajima, Y. *Chem. Mater. Commun.* **2004**, *16*, 3399.
(10) Nakayama, M.; Goto, S.; Uchimoto, Y.; Wakihara, M.; Kitajima, Y.; Miyanaga, T.; Watanabe, I. *J. Phys. Chem. B* **2005**, *109*, 11197.
(11) Augustsson, A;, Zhuang, G. V.; Butorin, S. M.; Osorio-Guillen, J. M.; Dong, C. L.; Ahuja, R.; Chang, C. L.; Ross, P. N.; Nordgren, J.; Guo, J.-H. *J. Chem. Phys.* **2005**, *123*, 184717.
(12) Shirakawa, J.; Nakayama, M.; Wakihara, M.; Uchimoto, Y. *J. Phys. Chem. B* **2006**, *110*, 17743.
(13) Uchimoto, Y.; Sawada, H.; Yao, T. *J. Synchrotron Radiat.* **2001**, *8*, 872. Uchimoto Y., Sawada, H.; Yao, T. *J. Power Sources* **2001**, *97-98*, 326.
(14) Kim, M.-G.; Lee, M.-K.; Shin, H.-J.; Lee, J.-M.; Lee, J.-S.; Yo, C.-H. *J. Phys. Chem. B* **2002**, *106*, 2526.
(15) Nakayama, M.; Imaki. K.; Ra, W.; Ikuta, H.; Uchimoto, Y.; Wakihara, M. *Chem. Mater.* **2003**, *15*, 1728.
(16) Nakayama, M.; Usui. T.; Uchimoto, Y.; Wakihara, M.; Yamamoto, M. *J. Phys. Chem. B* **2005**, *109*, 4143.
(17) Ra, W.; Nakayama, M.; Ikuta, H.; Uchimoto, Y.; Wakihara, M. *Appl. Phys. Lett.* **2004**, *84*, 4364.
(18) Ra, W.; Nakayama, M.; Ikuta, H.; Uchimoto, Y.; Wakihara, M. *J. Phys. Chem. B* **2005**, *109*, 1130.
(19) Ra, W.; Nakayama, M.; Cho, W.; Wakihara, M.; Uchimoto, Y. *Phys. Chem. Chem. Phys.* **2006**, *8*, 882.
(20) Kim, Y.; Izumi, F. *J. Ceram. Soc. Jpn.* **1994**, *102* (4), 401.
(21) Christidis, P. C.; Rentzeperis, P. J. *Z. Kristallogr., Kristallgeom., Kristallphys., Kristallchem.* **1976**, *144*, 341.
(22) Rapposch, M. H.; Anderson, J. B.; Kostiner, E. *Inorg. Chem.* **1980**, *19*, 3531.
(23) Reiff, W. M.; Zhang, J. H.; Torardi, C. C. *J. Solid State Chem.* **1986**, *62*, 231.
(24) Padhi, A. K.; Manivannan, V.; Goodehough, J. B. *J. Electrochem. Soc.* **1998**, *145*, 1518.
(25) Reiff, W. M.; Zhang, J. H.; Tam, H.; Attfield, J. P.; Torardi, C. C. *J. Solid State Chem.* **1997**, *130*, 147.
(26) Crocombette, J. P.; Pollak, M.; Jollet, F.; Thromat, N.; Gautier-Soyer, M. *Phys. Rev. B* **1995**, *52*, 3143.
(27) Bacq, O. L.; Pasturel, A.; Bengone, O. *Phys. Rev. B* **2004**, *70*, 245107.
(28) Bacq, O. L.; Pasturel, A. *Philos. Mag.* **2005**, *85*, 1747.
(29) Kuiper, P.; Kruizinga, G.; Ghijsen, J.; Sawatzky, G. A. *Phys. Rev. Lett.* **1989**, *62*, 221.
(30) Szilagyi, R. K.; Frank, P.; George, S. D.; Hedman, B.; Hodgson, K. *Inorg. Chem.* **2004**, *43*, 8318.
(31) Dathe, H.; Jentys, A.; Lercher, J. A. *J. Phys. Chem. B* **2005**, *109*, 21846.